Published in final edited form as:
Polymer (Guildf). 2011 August 18; 52(18): 3887–3896. doi:10.1016/j.polymer.2011.07.007.

Synthesis and Gelation Characteristics of Photo-Crosslinkable Star Poly(ethylene oxide-co-lactide-glycolide acrylate) Macromonomers

Seyedsina Moeinzadeh, **Saied Nouri Khorasani**, **Junyu Ma**, **Xuezhong He**, and **Esmaiel Jabbari**
Biomimetic Materials and Tissue Engineering Laboratories, Department of Chemical Engineering, University of South Carolina, Columbia, SC 29208

Abstract

Viability of encapsulated cells *in situ* crosslinkable macromonomers depends strongly on the minimum concentration of polymerization initiators and monomers required for gelation. Novel 4-arm poly(ethylene oxide-co-lactide-glycolide acrylate) (SPELGA) macromonomers were synthesized and characterized with respect to gelation, sol fraction, degradation, and swelling in aqueous solution. SPELGA macromonomers were crosslinked in the absence of N-vinyl-2-pyrrolidone (NVP) monomer to produce a hydrogel network with a shear modulus of 27±4 kPa. The shear modulus of the gels increased by 170-fold as the macromonomer concentration was increased from 10 to 25 wt%. Sol fraction ranged between 8–18%. Addition of only 0.4 mol% NVP to the polymerization mixture increased modulus by 2.2-fold from 27±4 (no NVP) to 60±10 kPa. The higher modulus was attributed to the dilution effect of polymer chains in the sol, by delaying the onset of diffusion-controlled reaction, and cross-propagation of the growing chains with network-bound SPELGA acrylates. Degradation of SPELGA gels depended on water content and density of hydrolytically degradable ester groups.

Keywords

star macromonomer; degradable; gelation kinetics

Introduction

A novel approach to tissue regeneration is the use of injectable *in situ* crosslinkable hydrogels as a carrier for the delivery of therapeutic agents and cells [1, 2]. Less invasive injectable gels coupled with minimally invasive arthroscopic techniques are an attractive alternative to implantation of pre-formed polymers for treating irregularly shaped or inaccessible defects [3–6]. Furthermore, diffusivity of nutrients [7, 8] and proteins [9, 10] in hydrogels is 4–5 orders of magnitude higher than solid polymers, thus providing a supportive matrix for differentiation, proliferation, and maturation of seeded cells into the

Corresponding author: Esmaiel Jabbari, Ph.D., Associate professor of Chemical Engineering, Department of Chemical Engineering, Swearingen Engineering Center, Rm 2C11, University of South Carolina, Columbia, SC 29208, Tel: (803) 777-8022, Fax: (803) 777-0973, jabbari@engr.sc.edu.

desired tissue [11]. In addition, hydrogels can be reinforced with calcium phosphate nanoparticles to produce injectable cements for hard tissue applications [1, 12, 13].

Biodegradable polymers are widely used as a supportive carrier in tissue engineering and drug delivery [14–18]. Among them, poly(lactide-co-glycolide) (PLGA) is the most widely used biodegradable polymer because its degradation products (lactic and glycolic acid) are resorbed through metabolic pathways [19, 20]. PLGA and poly(ε-caprolactone) (PCL) polymers have been copolymerized with poly(ethylene oxide) (PEO) to produce amphiphilic macromers that form thermally-induced physical gels [21–23]. Studies concerning the effect of macromer structure on water content and modulus [22, 24] demonstrate that physically crosslinked gels are significantly weaker than those that are chemically crosslinked [25, 26], limiting them for use in non-load bearing biomedical applications. In addition, degradability of chemically-crosslinked gels can be controlled independent of gelation by the molecular weight and ratio of hydrophobic/hydrophilic domains [21, 27, 28]. To control the hydrogel water content (and therefore mechanical strength), degradation rate and the rate of crosslinking, our laboratory has previously developed a poly(lactide-co-ethylene oxide fumarate) (PLEOF) macromonomer consisting of low molecular weight poly(L-lactide) (LMW-PLA) and PEG blocks linked by unsaturated fumarate units [6, 26]. The water content of the PLEOF hydrogel could be adjusted by the ratio of hydrophilic PEG to hydrophobic PLA blocks and by PEG molecular weight [26]. Degradation rate of the network could be controlled by the ratio of PLA to PEG blocks or by the molecular weight of PLA segments [26]. However, due to steric hindrance of the fumarate groups along the chain and their lower reactivity (compared to acrylates and methacrylates) [26, 29, 30], the gelation kinetics depended strongly on UV initiator and small molecule monomer concentrations [26]. It is well established that the viability of cells encapsulated in synthetic gels is largely determined by the fraction of small-molecule initiators and monomers that cross the cell membrane [31, 32].

Terminal reactive groups at chain ends are less sterically hindered compared to those along the macromonomer chain. The reactivity of acrylates is an order of magnitude higher than fumarates [6, 26, 33]. In addition, star macromonomers have lower shear viscosity than linear ones at the same molecular weight [34], resulting in the onset of gelation at higher conversions and a higher extent of crosslinking. We hypothesized that a multi-arm star amphiphilic poly(ethylene oxide-co-lactide-glycolide) based macromonomer each arm terminated with an acrylate group would significantly increase the rate of crosslinking, thus reducing the minimum required concentration of initiator/monomer to produce robust networks. The objective of this work was to synthesize a novel star poly(ethylene oxide-co-lactide-glycolide acrylate) (SPELGA) macromonomer and investigate the effect composition had on gelation kinetics and degradation of the hydrogels. In this work, SPELGA macromonomer was synthesized by ring-opening polymerization of lactide and glycolide monomers using hydrophilic pentaerythritol ethoxylate or poly(ethylene glycol) initiators, followed by acrylation of the chain ends with acryloyl chloride. The structure of the synthesized macromonomers was characterized by ^{1}H-NMR and GPC. The kinetics of photopolymerization of the SPELGA macromonomers in aqueous solution was investigated by rheometry. The SPELGA hydrogels were characterized with respect to sol fraction, swelling and degradation.

Experimental

1. Materials

Lactide (LA; >99.5% purity by GPC) and glycolide (GL; >90% purity) monomers were purchased from Ortec (Easley, SC) and Boehringer Chemicals (Ingelheim, Germany), respectively. The ring opening polymerization initiators 4-arm pentaerythritol ethoxylate

(PEE800; 15/4 EO/OH; M_n=797 Da; purity >98%) and 4-arm poly(ethylene glycol) (4PEG5K; nominal molecular weight of 5 kDa; purity >98%) were purchased from Sigma-Aldrich (St. Louis, MO), respectively. The initiators were dried by azeotropic distillation from toluene prior to the reaction. Triethylamine (TEA), tin (II) 2-ethylhexanoate (TOC), N-vinyl-2-pyrrolidone (NVP), and acryloyl chloride were purchased from Sigma-Aldrich. Methylene chloride (MC; VWR) was dried by distillation over calcium hydride (Sigma-Aldrich). All other solvents were reagent grade and used as received.

2. Synthesis of SPELGA macromonomer

Star poly(ethylene oxide-co-lactide-glycolide) (SPELG) macromer was synthesized by ring-opening polymerization of LA and GA monomers with star 4PEE800 or 4PEG5K initiators, following a procedure similar to the synthesis of low molecular weight poly(L-lactide) [6, 35, 36]. The schematic diagram for the synthesis of SPELG with 4PEE800 is shown in Figure 1. TOC was used as the polymerization catalyst and LA/GL ratio was 100/0 for SPELGA-5K and 100/0, 75/25, 50/50 for SPELGA-800. In a typical procedure for the synthesis of 100/0 SPELGA, 30g LA (0.2084 mol) and 0.0116 mol initiator (7 ml 4PEE800 or 58 g 4PEG5K) were added to a three-neck reaction flask equipped with an overhead stirrer. The reaction flask was submerged in an oil bath and gradually heated to 110–120°C to melt the monomers while under steady flow of nitrogen. After melting, 3 ml TOC as the polymerization catalyst was added to the reaction mixture with stirring. The reaction was allowed to proceed for 6 h at 135°C. Upon completion, the product was dissolved in DCM and precipitated in ice cold methanol, ether, and hexane to fractionate the PLA product and remove the unreacted monomer and initiator [35]. The solvent was decanted and the star SPELG product was vacuum dried (<5 mmHg) to remove any residual solvent and stored at −20°C. With TEA as the reaction catalyst, the chain ends of the star SPELG were acrylated by the reaction of acryloyl chloride with the hydroxyl end-groups of the SPELG (see Figure 1). Prior to this reaction the SPELG macromer was dried by azeotropic distillation from toluene to remove residual moisture. The polymer was cooled under steady flow of nitrogen and dissolved in dried DCM. The reaction flask was immersed in an ice bath to limit a temperature rise from the exothermic reaction. In a typical reaction 5.6 ml acryloyl chloride and 9.7 ml TEA, each dissolved in DCM, were added drop-wise to the reaction with stirring. The reaction was allowed to proceed for 12 h under nitrogen flow. After completion of the reaction the solvent was removed by rotary evaporation and the residue was dissolved in anhydrous ethyl acetate to precipitate the by-product triethylamine hydrochloride salt. Next, ethyl acetate was removed by vacuum distillation; the macromonomer was re-dissolved in DCM and precipitated twice in ice cold ethyl ether. The macromonomer was dissolved in dimethylsulfoxide (DMSO) and further purified by dialysis to remove any unreacted acrylic acid. The SPELGA product was dried in vacuum (<5 mmHg) to remove residual solvent and stored at −20°C.

3. Macromonomer characterization

The chemical structure of the SPELGA macromonomer was characterized by a Varian Mercury-300 ^{1}H-NMR (Varian, Palo Alto, CA) at ambient conditions with a resolution of 0.17 Hz as described [6]. The sample was dissolved in deuterated chloroform (Sigma-Aldrich, 99.8% deuterated) at a concentration of 50 mg/ml, and 1% v/v trimethylsilane (TMS; Sigma-Aldrich) was used as the internal standard. The molecular weight distribution of the macromonomer was measured by GPC [6]. Measurements were carried out with a Waters 717 Plus Autosampler GPC system (Waters, Milford, MA) connected to a model 616 HPLC pump, model 600S controller, and a model 410 refractive index detector. The columns consisted of a styragel HT guard column (7.8 × 300 mm, Waters) in series with a styragel HR 4E column (7.8 × 300 mm, Waters) heated to 37°C in a column heater. The Empower software was used for determination of number $(\overline{M_n})$ and weight $(\overline{M_w})$ average

molecular weights and polydispersity index (PI). The sample (20 μl) with a concentration of 10 mg/ml in tetrahydrofuran (THF) was eluted with degassed THF at a flow rate of 1 ml/min. Monodisperse polystyrene standards (Waters) with peak molecular weights (M_p) of 0.58–19.9, 66.35, and 143.4 kDa and polydispersities of <1.1 were used to construct the calibration curve.

4. SPELGA gelation

The SPELGA macromonomer was crosslinked in aqueous solution by free-radical UV polymerization with 4-(2-hydroxyethoxy) phenyl-(2-hydroxy-2-propyl) ketone (Irgacure 2959; CIBA, Tarrytown, NY) photo-initiator [13, 26, 33]. The photo-initiator was dissolved in distilled deionized (DI) water at 50°C. The SPELGA macromonomer was dissolved in DI water by vortexing and heating to 50°C to aid dissolution. The initiator solution was added to the SPELGA solution, this mixture was then vortexed and loaded on the Peltier plate of the rheometer. To make 10, 15, and 20% SPELGA precursor solution, 30, 45, and 60 mg of the macromonomer solution was added to 270, 255 and 240 ml of the initiator solution, respectively. In samples with NVP added as a crosslinking agent, the initiator was first dissolved in the desired amount of NVP before addition to the macromonomer solution. The sample was irradiated with a BLAK-RAY 100-W mercury long wavelength (365 nm) UV lamp (Model B100-AP; UVP, Upland, CA) [26]. The notation “SPELGAa-Lb-Mc-Nd-Ie” is used to identify the composition of the samples, where a, b, c, d and e represent initiator molecular weight, lactide fraction and macromonomer molecular weight, NVP and initiator concentrations (wt%), respectively. The results are for SPELGA, NVP and initiator concentrations of 25 wt%, 0 mol%, and 0.16 mol%, respectively, unless otherwise specified.

5. Rheological measurements

Rheological measurements were carried out at 37°C on an AR-2000 rheometer (TA Instruments, New Castle, DE) equipped with a parallel plate geometry (acrylic plate transparent to UV light; 20 mm diameter; TA Instruments) [26]. A sinusoidal shear strain profile was exerted on the sample via the upper geometry at a constant frequency of 1 Hz. The deformation amplitude was kept at 1% to remain within the linear viscoelastic region. The polymerizing mixture was injected on the Peltier plate and the upper geometry was lowered to a gap of 500 μm. The sample was irradiated with a long wavelength UV lamp (Model B100-AP; UVP, Upland, CA) as described above. The elapsed time between mixing/injection and the start of data collection was ≤1 min for all experiments. The storage modulus (G’) during the gelation process was monitored by the rheometer. The intensity of the transmitted UV light was measured by a BLAK-RAY long wave ultraviolet radiation meter (Model J-221; UVP). The transparency of the acrylic geometry to long wave (365nm) UV light was confirmed by comparing the intensity of the transmitted light through the geometry to the incident light (transmitted intensity was >95%). The measured UV intensities at distances of 10, 30, 35, and 40 cm from the lamp were 46,000, 5,300, 4,000, and 3,000 μW/cm^2, respectively. We have previously shown that a UV intensity of 46,000 μW/cm^2 applied 10 cm from the sample and exposure time of 1800 s results in the highest extent of crosslinking [26]. Therefore, all gelation results are with UV intensity, distance, and exposure time of 46,000 μW/cm^2, 10 cm, and 1800 s, respectively. In the text,”modulus” is defined as the storage shear modulus of the sample after 1800 s of UV radiation.

6. Measurement of swelling ratio and sol fraction

After crosslinking, samples with dimensions 20 mm diameter × 300 μm thickness were removed from the Peltier plate to measure their swelling ratio and sol fraction. Samples were dried at ambient conditions for 12 h followed by drying in vacuum for 1 h at 40°C and the total dry weights (W_i) were recorded. Next, dry samples were swollen in DI water for 24 h at

37°C and swelling medium changed every 6 h. After swelling the surface water was removed and the swollen weight (W_s) was recorded. Then, the swollen samples were dried as described above and the dry weight (W_d) were recorded. The weight swelling ratio (Q) and sol fraction (S) were calculated by the following equations:

$$Q = \frac{W_s - W_d}{W_d} \times 100 \quad (1)$$

$$S = \frac{W_i - W_d}{W_i} \times 100 \quad (2)$$

7. Measurement of degradation

The SPELGA precursor solution was degassed, transferred into a PTFE mold (3cm × 5cm × 750μm), covered with a transparent glass plate fastened with clips, and UV crosslinked as described above. After crosslinking the sample was removed from the mold and disks were cut from the gel using an 8 mm cork borer. Degradation was measured as a function of time in primary culture media (5 ml per sample) without fetal bovine serum (FBS) at 37°C under mild agitation. To prepare the primary media 13.4 g of Dulbecco's Modified Eagle Medium (DMEM; 4.5 g/l glucose with L-glutamine and without sodium pyruvate; Mediatech, Herndon, VA) was dissolved in 900 ml of DI water containing 3.7 g sodium bicarbonate and 10 ml antibiotic and antimycotic agent (1% v/v). At each time point samples were removed from the media, rinsed with DI water to remove excess electrolytes, and dried under vacuum. The dry sample weight was recorded and compared with the initial dry weight to determine fractional mass remaining with respect to time.

Results

The ^{1}H-NMR spectrum of SPELGA800-L50 is shown in Figure 2. The chemical shifts with peak positions at 1.6 and 5.2 ppm were attributed to the methyl (−CH_3) and methine (≡CH) hydrogens of the lactide units in SPELGA, respectively [37]. The shift centered at 4.8 ppm was attributed to the methylene hydrogens (=CH_2) of the glycolide units in SPELGA. The shifts centered at 3.6 and 4.3 ppm were attributed to the methylene hydrogens (=CH_2) of the 4-arm initiator (4PEE800 or 4PEG5K) attached to the ether (−CH_2-O-CH_2-) and ester (−CH_2-OOC-) groups of lactide/glycolide units, respectively [37]. The chemical shifts with peak positions from 5.85–6.55 ppm were attributed to the vinyl hydrogens of the acrylate groups (−CH=CH2) at chain ends; the latter shifts were absent in the spectra of unacrylated SPELG (see the inset of Figure 2). The relative intensities of the NMR shifts of SPELGA macromonomers are presented in Table 1. The ratio of the shifts centered at 1.6 and 5.2 ppm (lactide hydrogens) to that at 4.8 ppm (glycolide hydrogens) was related to the molar ratio of LA/GL. The ratio of the shifts centered at 1.6, 5.2, and 4.8 (lactide+glycolide hydrogens) to those at 3.6 and 4.3 ppm (4-arm initiator hydrogens) was related to $\overline{M_n}$ of SPELGA. The ratio of the shifts centered at 5.85–6.55 ppm (acrylate hydrogens) to those at 3.6 and 4.2 ppm (initiator hydrogens) was related to the average number of acrylate groups per macromonomer. The LA/GL molar ratio, $\overline{M_n}$, and the number of acrylate groups per SPELGA800 calculated from the NMR data are given in Table 1. For SPELGA800-L50 and SPELGA800-L75 with feed LA/GL ratios of 1.0 and 3.0, respectively, the actual ratios from the NMR data were 1.2 and 3.4. The actual LA/GL ratio was slightly higher than the feed indicating that the reactivity of lactide monomer with the growing chain was slightly higher than that of glycolide. The number of acrylate groups per macromonomer for SPELGA800-L50 and SPELGA800-L75 were 3.2 and 3.6, respectively.

$\overline{M_n}$, $\overline{M_w}$, and PI of the synthesized SPELGA macromonomers which were measured by GPC are presented in Table 2. $\overline{M_n}$, $\overline{M_w}$, and PI of SPELGA800 were independent of LA/GL ratio. SPELGA5K, due to higher PEG chain length, had the highest molecular weight and lowest PI. The $\overline{M_n}$ values measured by GPC were within 10% of the values calculated from the intensity of NMR shifts. All SPELGA macromonomers were dissolved in water, heated to 50°C and crosslinked into a hydrogel. The SPELGA800-L100 with low PEG molecular weight and 100% hydrophobic lactide fraction was not used in the subsequent gelation experiments due to its low solubility in aqueous solution. SPELGA5K-L100 had the highest solubility in water as measured by a turbidity test (data not shown).

To determine the effect of UV initiator on crosslinking, the gelation kinetics of SPELGA5K-L100-M25-N0 macromonomer were monitored by rheometry and the results are shown in Figure 3. As the initiator concentration was increased from zero to 0.11, 0.16, and 0.22 mol %, modulus increased from 1.3±0.3 to 10.0±2.1, 27.1±4.1, and 23.6±4.7, respectively. G' initially increased for up to 0.16 mol% initiator concentration and then decreased for >0.16 mol% concentration. Figures 4a and 4b show the effect of macromonomer concentration (based on the weight of polymerizing mixture) on the modulus and sol fraction of SPELGA5K-L100-N0-I0.16 gels, respectively. SPELGA5K, due to its higher solubility in water, was selected to study the effect of macromonomer concentration. There was a continuous increase in G' with increasing macromonomer concentration. G' increased from 0.16±0.03 to 0.47±0.12, 3.4±0.4, 5.9±1.0, 6.9±0.9, 13.4±2.4, and 27.1±4.1 kPa as the macromonomer concentrations increased from 10 to 12.5, 15, 17.5, 20, 22.5, and 25 wt%, respectively, with 170-fold overall increase in modulus. Sol fraction decreased from 17.8±1.1 to 15.6±1.5, 12.2±1.6, 13.8±3.0, 12.0±1.2, 9.4±0.9, and 7.6±0.9% as the macromonomer concentration increased from 10 to 12.5, 15, 17.5, 20, 22.5, and 25 wt%, respectively. The sol fraction of the PLEOF hydrogel with and without NVP monomer is also shown in Figure 4b. SPELGA macromonomers with higher reactivity and lower steric hindrance of the acrylate groups had significantly lower sol fraction (S=8–18% in the absence of NVP) compared to PLEOF without (S=71%) or with (S=39%) NVP. It is well-established that the diffusivity/mobility of the growing chain affects gelation and the extent of crosslinking [26, 38]. Therefore, NVP was used to investigate the effect of a small molecule monomer on the plateau shear modulus of SPELGA hydrogels. Figures 5a and 5b show the effect of NVP concentration on the evolution and plateau modulus of SPELGA5K-L100-M25-I0.16 hydrogels, respectively. Addition of only 0.4 mol% NVP (0.004 moles NVP per mole of solution) to the polymerization mixture increased the modulus 2.2-fold from 27±4 (no NVP) to 60±10 kPa but the modulus did not change appreciably for concentrations >0.4 mol%. The gelation time of the samples was <60 s for all NVP fractions (50, 35, and 41 s for zero, 0.4, and 0.61% NVP, respectively). Based on Figure 5a, addition of 0.4 mol% NVP affected modulus after the gelation point, but the curves were almost identical for higher NVP fractions. The effect of initiator molecular weight and LA/GL ratio of SPELGA-M15 on modulus is shown in Figure 6. SPELGA5K had a significantly lower modulus (3.3±0.4 kPa) compared to SPELGA800 (11.6±3.0 and 15.4±3.2 for SPELGA800-L75 and SPELGA800-L50, respectively). This can be attributed to the higher molecular weight of SPELGA5K compared to SPELGA800, resulting in lower density of reactive acrylate groups in the sample.

The effect of initiator molecular weight and LA/GL ratio on sample mass loss and swelling ratio is shown in Figures 7a and 7b, respectively. SPELGA800-L50 with the highest content of the less hydrophobic glycolide monomer had the highest mass loss over a period of 7 weeks, followed by SPELGA5K-L100 and SPELGA800-L75. For example, after 4 weeks, SPELGA800-L50, SPELGA5K-L100, and SPELGA800-L75 lost 50.0±7.7, 33.0±1.9, and 23±0.4% mass, respectively. The swelling ratios support the mass loss results with

SPELGA5K and SPELGA800-L75 showing the highest and lowest water contents, respectively. For example, after 4 weeks SPELGA5K-L100, SPELGA800-L50, and SPELGA800-L75 had swelling ratios of 645, 43, and 7%, respectively, corresponding to water fractions of 87, 30, and 6 wt%. Interestingly, SPELGA800 hydrogel showed delayed swelling characteristics, which could potentially be useful for the design of delayed drug release systems. For example, SPELGA800-L50 and SPELGA800-L75 had only 5.7 and 3.8 wt% water content after 4 weeks of incubation; however, their water content increased to 83 and 11 wt% after 7 weeks.

Discussion

SPELGA macromonomers crosslinked in the absence of NVP (see Figure 5) produced a relatively high modulus hydrogel (27±4 kPa). The results in Figures 3 and 5 demonstrate that initiator and NVP concentrations as low as 0.16 and 0.4 mol%, respectively, produced hydrogels with >10 kPa shear modulus. It should be noted that the initiator and NVP concentrations used in this study were an order of magnitude lower than those used for gelation of the linear PLEOF macromonomer [26]. The higher reactivity of the acrylates in SPELGA compared to fumarates in linear PLEOF reduced the minimum required concentration of the initiator and NVP to produce robust networks. It is well established that the viability of cells encapsulated in hydrogels depends strongly on the concentration of small molecule initiator and monomer that can cross the cell membrane. Therefore, the lower initiator and NVP concentrations required for gelation has potential to improve biocompatibility of SPELGA hydrogels for cell encapsulation.

The modulus initially increased with initiator concentration for up to 0.16 mol% and then decreased at higher fractions. The dependence of propagation rate, R_P, on initiator concentration in the absence of NVP is given by [39]:

$$R_p = k_{P,AC}\,[AC]\left[\frac{R_{i,AC}}{k_t}\right]^{1/2} = k_{P,AC}\,[AC]\left[\frac{\phi\varepsilon I_0\delta[I]}{k_t}\right]^{1/2} \quad (3)$$

where $k_{P,AC}$ and k_t are the rate constant for chain propagation and termination, $R_{i,AC}$ is the radical initiation rate, [*AC*] is the concentration of unreacted SPELGA acrylates, ϕ is photo-initiation efficiency, ε is molar extinction coefficient, I_0 is incident radiation intensity, δ is gel thickness, and [*I*] is the initiator concentration. Higher initiator concentrations below 0.16 mol% increased the rate of propagation, leading to a hydrogel with higher network density and higher modulus, as shown in Figure 3. At concentrations above 0.16 mol%, although the propagation rate continued to increase, there was a higher probability of localized formation of multiple radicals on growing chains, leading to cluster formation and increased cyclization within those clusters. This premise is supported by the decrease in gelation time from 460 s to 100, 50 and <30 s, as the initiator concentration was increased from zero to 0.11, 0.16, and 0.22 mole%, respectively. The increased cyclization and cluster formation reduced the modulus at initiator concentrations >0.16 mol%. Wang and collaborators observed a similar effect when UV intensity was increased above a threshold level in UV photocrosslinked polyacrylamide gels [40]. Similarly, a reduction in tensile modulus above a certain initiator concentration was reported for multi-functional methacrylamide, poly(ethylene glycol), and N-vinyl pyrrolidone hydrogels [41]. Results in Figure 3 indicate that the optimum initiator concentration in the absence of NVP was 0.16 mol%.

The addition of NVP monomer increased the hydrogel modulus, as shown in Figure 5. At any time there are monomers, linear and branched chains and a gel network in the

polymerization reaction. The four propagation reactions involving the acrylate groups of NVP monomer and SPELGA macromonomer are given by:

$$\sim X^{*}+NVP \xrightarrow{k_{P,Vs}} \sim NVP^{*} \tag{4}$$

$$\sim X^{*}+AC \xrightarrow{k_{P,As}} \sim AC^{*} \tag{5}$$

$$>X^{*}+NVP \xrightarrow{k_{P,Vg}} >NVP^{*} \tag{6}$$

$$>X^{*}+AC \xrightarrow{k_{P,Ag}} >AC^{*} \tag{7}$$

Where [NVP] and [AC] are concentrations of unsaturated vinyl groups of NVP and SPELGA, respectively, and symbols "~" and ">" denote a linear or branch chain in the sol (not part of the network) and the gel, respectively. For example, $\sim X^{*}$ is a growing chain in the sol with a radical attached to X terminal group, with X being NVP ($\sim NVP^{*}$) or SPELGA acrylate ($\sim AC^{*}$). Symbol $>X^{*}$ denotes a growing chain in the gel with a radical attached to X terminal group. There are also four propagation reactions involving unreacted acrylates of those SPELGA macromonomers that are part of a chain in the sol or the gel (~AC or >AC), which are given by:

$$\sim X^{*}+\sim AC \xrightarrow{k_{P,br}} \sim AC^{*}+br \tag{8}$$

$$\sim X^{*}+>AC \xrightarrow{k_{P,dc1}} >AC^{*}+d.c. \tag{9}$$

$$>X^{*}+\sim AC \xrightarrow{k_{P,dc2}} >AC^{*}+d.c. \tag{10}$$

$$>X^{*}+>AC \xrightarrow{k_{P,nc}} >AC^{*}+n.c. \tag{11}$$

Notation "br" stands for a branch in a chain (not part of the gel). Notations "d.c." and "n.c." denote a dangling (non-load bearing) and a network (load bearing) chain, respectively. In propagation reactions (4) and (5), a growing radical in the sol ($\sim X^{*}$) reacts with an NVP and SPELGA monomer, respectively, with rate constants $k_{P,Vs}$ and $k_{P,As}$. Reactions (4) and (5) produce linear or branched polymer chains that dilute the hydrogel network. In propagation reactions (6) and (7), a growing radical in the network ($>X^{*}$) reacts with an NVP monomer and SPELGA macromonomer, respectively, with rate constants $k_{P,Vg}$ and $k_{P,Ag}$, forming dangling radical chains in the network. In reaction (8), a growing radical in the sol reacts with a SPELGA acrylate that is part of a chain in the sol (~AC) with rate constant $K_{P,br}$, thus adding a branch to the chain. Reactions (9) and (10) form dangling chains attached to the gel by the reaction of a growing radical in the sol with a SPELGA acrylate in the gel ($>AC^{*}$;

rate constant $k_{P,dc1}$) or by the reaction of a growing radical in the gel with a SPELGA acrylate on a chain in the sol (~AC, rate constant $k_{P,dc2}$). In reaction (11), a growing radical in the network (>X^*) reacts with a SPELGA acrylate in the network (>AC) with rate constant $k_{P,nc}$ forming a network chain, as shown in Figure 8. Since the ratio of NVP/SPELGA vinyl groups for 0.4, 0.61, and 0.83 mol% NVP is 1.3, 2.1, and 2.7, respectively, reactions (4) through (11) all contribute to the polymerization and gelation.

Reactions (4), (5), and (8) produce polymer chains in the sol which act as diluents and delay the onset of diffusion-controlled polymerization. The delay potentially reduces the trapping of reactive acrylate groups in localized SPELGA clusters. This increases the overall conversion, resulting in a higher storage modulus as shown in Figure 5. Nowers and collaborators observed a similar effect when acrylated poly(ethylene glycol) (PEG) was added to epoxy polymerization [42]. Reactions (6) and (7) are propagation reactions between a growing radical on the network with NVP monomer and SPELGA macromonomer, respectively. In reactions (9) and (10), a growing radical on the network cross-propagates with a SPELGA acrylate on a chain in the sol, or a growing radical in the sol cross-propagates with a SPELGA acrylate on the network to form a dangling chain attached to the network. In reaction (11), a growing radical on the network (>X^*) reacts with a network-bound SPELGA acrylate to form a load-bearing crosslink point (see Figure 8), leading to a hydrogel with a higher modulus (Figure 5). As the NVP fraction is increased beyond a certain value, the delay in the onset of diffusion-controlled polymerization counteracts the dilution effect of polymer chains in the sol. Ultimately, this leads to no further increase in modulus (see Figure 5 for 0.4, 0.61, and 0.83 mol% NVP). Since the diffusivities of NVP monomer and NVP-rich growing chains (reactions 4 and 6) are relatively higher those that of SPELGA macromonomer and SPELGA-rich growing chains (reactions 5 and 7), the propagation reactions (6) and (7) and the cross-propagation reactions (9) and (10) serve as a bridge between the network-bound SPELGA acrylates to increase the number of network density. Therefore, the higher modulus of the hydrogels in the presence of NVP can be explained by the dilution effect of polymer chain in the sol to delay the onset of diffusion-controlled reaction, and by propagation of NVP monomer and growing chains with network-bound SPELGA acrylates to facilitate crosslinking.

The average molecular weight between crosslinks, $\overline{M_c}$, can be determined by the equation for rubber elasticity [43]:

$$\overline{M_c} = RT\frac{\rho}{G'}(1 - S) \tag{5}$$

Where ρ is the macromonomer mass density (1100 kg/m^3), G' is modulus (Pa), R is gas constant (8.31 J/mol K), T is absolute temperature (310 K), and S is sol fraction (see Eq. 2 and data in Figure 4b). Using Eq. (5), $\overline{M_c}$ decreased from 97 ± 12 to 43 ± 5 kDa as the NVP concentration was increased from 0 to 3.6 wt% for SPELGA5K-L100-P25-I0.16 hydrogel.

Degradation of SPELGA gels depends on the gel water content and density of hydrolytically degradable ester linkages. The relatively fast degradation of SPELGA800-L50 can be contributed to the high density of degradable LA/GL units (70% LA/GL and 30% 4PEE800), higher content of less hydrophobic glycolide monomer (50% by weight), and the autocatalytic effect of acidic degradation products [44]. SPELGA5K-L100 with 76% by weight PEG content had high water content (540 wt% swelling ratio after 1 week as shown in Figure 7b) but low density of degradable lactide units (24%), resulting in a degradation rate lower than that of SPELGA800-L50. SPELGA800-L75 with a high density of more

hydrophobic lactide groups and low water content (see Figure 7b) exhibited the lowest mass loss with time.

Conclusion

A novel star poly(ethylene oxide-co-lactide-glycolide acrylate) (SPELGA) macromonomer was synthesized and characterized with respect to gelation, sol fraction, degradation, and swelling in aqueous solution. We hypothesized that a multi-arm star amphiphilic poly(ethylene oxide-co-lactide-glycolide) based macromonomer with each arm terminated with an acrylate group would significantly increase the rate of crosslinking, thus reducing the minimum required concentration of initiator/monomer to produce robust networks. Addition of only 0.4 mol% NVP to the polymerization mixture increased modulus by 2.2-fold but modulus did not change appreciably for higher NVP concentrations. The higher modulus can be explained by the dilution effect of polymer chains in the sol, to delay the onset of diffusion-controlled reaction, and by propagation of growing polymer chains with network-bound SPELGA acrylates to facilitate network formation. It is interesting to note that the minimum NVP concentration of 0.4% was at least an order of magnitude less than that used in previous studies for gelation of PLEOF macromonomers. Depending on macromonomer concentration, sol fraction ranged between 8–18%. The higher reactivity and lower steric hindrance of the acrylates in SPELGA compared to fumarates in PLEOF significantly reduced sol fraction and minimum NVP concentration to produce robust networks. SPELGA gels with highest LA/GL content (SPELGA800-L50) had the highest mass loss but lowest water uptake with incubation time which was attributed to the high fraction of degradable units and the autocatalytic effect of acidic degradation products. SPELGA gels with highest LA/GL content (SPELGA800-L75 and SPELGA800-L50) showed delayed swelling characteristics.

Acknowledgments

This work was supported by research grants to E. Jabbari from the National Science Foundation under grant Nos. CBET0756394, CBET0931998, and DMR1049381, the National Institutes of Health under Grant No. DE19180, and the Arbeitsgemeinschaft Fur Osteosynthesefragen (AO) Foundation under Grant No. C10-44J. S.N. Khorasani likes to acknowledge the financial support of Isfahan University of Technology for a sabbatical award to him for a visiting professorship at the University of South Carolina. The authors like to thank Dr. Weijie Xu and Mr. Jianping Wu (Chemical Engineering) for assistance with polymer synthesis. The authors thank Ms. Leah Pruzinsky for editing the manuscript.

References

1. Zhao LA, Weir MD, Xu HHK. An injectable calcium phosphate-alginate hydrogelumbilical cord mesenchymal stem cell paste for bone tissue engineering. Biomaterials. 2010; 31:6502–6510. [PubMed: 20570346]
2. Jabbari, E.; Lu, L.; Currier, B.; Mikos, A.; Yaszemski, M. Injectable polymers and hydrogels for orthopedic and dental applications. In: Sandell, L.; Grodzinsky, A., editors. Tissue engineering in musculoskeletal clinical practice. Rosemont: American Academy of Orthopaedic Surgeons; 2004.
3. Wang HB, Zhou J, Liu ZQ, Wang CY. Injectable cardiac tissue engineering for the treatment of myocardial infarction. J Cell Mol Med. 2010; 14:1044–1055. [PubMed: 20193036]
4. Ballios BG, Cooke MJ, van der Kooy D, Shoichet MS. A hydrogel-based stem cell delivery system to treat retinal degenerative diseases. Biomaterials. 2010; 31:2555–2564. [PubMed: 20056272]
5. Cheng YH, Yang SH, Su WY, Chen YC, Yang KC, Cheng WTK, Wu SC, Lin FH. Thermosensitive chitosan-gelatin-glycerol phosphate hydrogels as a cell carrier for nucleus pulposus regeneration: An in vitro study. Tissue Eng. 2010A; 16:695–703.
6. He X, Jabbari E. Material properties and cytocompatibility of injectable MMP degradable poly(lactide ethylene oxide fumarate) hydrogel as a carrier for marrow stromal cells. Biomacromolecules. 2007; 8:780–792. [PubMed: 17295540]

7. Dembczynski R, Jankowski T. Characterisation of small molecules diffusion in hydrogelmembrane liquid-core capsules. Biochem Eng J. 2000; 6:41–44. [PubMed: 10908867]
8. Beruto DT, Botter R. Role of the water matric potential (psi(M)) and of equilibrium water content (EWC) on the water self-diffusion coefficient and on the oxygen permeability in hydrogel contact lenses. Biomaterials. 2004; 25:2877–2883. [PubMed: 14962566]
9. Peppas, NA.; Lustig, SR. Solute diffusion in hydrophilic network structures. In: Fundumentals, I.; Peppas, NA., editors. Hydrogels in medicine and pharmacy. Boca Raton: CRC Press; 1986. p. 57-84.
10. Liang S, Xu J, Weng L, Dai H, Zhang X, Zhang L. Protein diffusion in agarose hydrogel in situ measured by improved refractive index method. J Contr Rel. 2006; 115:189–196.
11. Saadi T, Arish A, Carmel J, Bramnik Z, Nayshool O, Mironi-Harpaz I, Seliktar D, Baruch Y. Hepatocyte cell line function in a biosynthetic hydrogel scaffold for liver tissue engineering. Liver Transplant. 2010; 16:S122–S122.
12. Sarvestani AS, He X, Jabbari E. Effect of osteonectin-derived peptide on the viscoelasticity of hydrogel/apatite nanocomposite scaffolds. Biopolymers. 2007; 85:370–378. [PubMed: 17183515]
13. Sarvestani AS, Jabbari E. Modeling and experimental investigation of rheological properties of injectable poly(lactide ethylene oxide fumarate)/hydroxyapatite nanocomposites. Biomacromolecules. 2006; 7:1573–1580. [PubMed: 16677041]
14. Pang XA, Chu CC. Synthesis, characterization and biodegradation of poly(ester amide)s based hydrogels. Polymer. 2010; 51:4200–4210.
15. Nair LS, Laurencin CT. Biodegradable polymers as biomaterials. Prog Polym Sci. 2007; 32:762–798.
16. Chan G, Mooney DJ. New materials for tissue engineering: towards greater control over the biological response. Trends Biotech. 2008; 26:382–392.
17. Puppi D, Chiellini F, Piras AM, Chiellini E. Polymeric materials for bone and cartilage repair. Prog Polym Sci. 2010; 35:403–440.
18. Ifkovits JL, Burdick JA. Photopolymerizable and degradable biomaterials for tissue engineering applications. Tissue Eng. 2007; 13:2369–2385. [PubMed: 17658993]
19. Miller ON, Bazzano G. Propanediol metabolism and its relation to lactic acid metabolism. Ann N Y Acad Sci. 1965; 119:957–973. [PubMed: 4285478]
20. Sodergard A, Stolt M. Properties of lactic acid based polymers and their correlation with composition. Prog Polym Sci. 2002; 27:1123–1163.
21. Jeong KJ, Panitch A. Interplay between Covalent and Physical Interactions within Environment Sensitive Hydrogels. Biomacromolecules. 2009; 10:1090–1099. [PubMed: 19301930]
22. Buwalda SJ, Dijkstra PJ, Calucci L, Forte C, Feijen J. Influence of amide versus ester linkages on the properties of eight-armed PEG-PLA star block copolymer hydrogels. Biomacromolecules. 2010; 11:224–232. [PubMed: 19938809]
23. Park SY, Han BR, Na KM, Han DK, Kim SC. Micellization and gelation of aqueous solutions of star-shaped PLLA-PEO block copolymers. Macromolecules. 2003; 36:4115–4124.
24. Lin HH, Cheng YL. In-situ thermoreversible gelation of block and star copolymers of poly(ethylene glycol) and poly(N-isopropylacrylamide) of varying architectures. Macromolecules. 2001; 34:3710–3715.
25. Amsden BG, Misra G, Gu F, Younes HM. Synthesis and characterization of a photo-cross-linked biodegradable elastomer. Biomacromolecules. 2004; 5:2479–2486. [PubMed: 15530066]
26. Sarvestani AS, Xu W, He X, Jabbari E. Gelation and degradation characteristics of in-situ photo-crosslinked poly(l-lactide-co-ethylene oxide-co-fumarate) hydrogels. Polymer. 2007; 48:7113–7120.
27. Salaam LE, Dean D, Bray TL. In vitro degradation behavior of biodegradable 4-star micelles. Polymer. 2006; 47:310–318.
28. Bae YH, Huh KM, Kim Y, Park KH. Biodegradable amphiphilic multiblock copolymers and their implications for biomedical applications. J Contr Rel. 2000; 64:3–13.

29. Oberti TG, Cortizo MS, Alessandrini JL. Novel copolymer of diisopropyl fumarate and benzyl acrylate synthesized under microwave energy and ouasielastic light scattering measurements. J Macromol Sci - Pure Appl Chem. 2010; 47:725–731.
30. Wei HY, Lee TY, Miao WJ, Fortenberry R, Magers DH, Hait S, Guymon AC, Jonsson SE, Hoyle CE. Characterization and photopolymerization of divinyl fumarate. Macromolecules. 2007; 40:6172–6180.
31. Lee PJ, Langer R, Shastri VP. Role of n-methyl pyrrolidone in the enhancement of aqueous phase transdermal transport. J Pharm Sci. 2005; 94:912–917. [PubMed: 15736187]
32. Xu QM, Cheng JS, Ge ZQ, Yuan YJ. Effects of organic solvents on membrane of Taxus cuspidata cells in two-liquid-phase cultures. Plant Cell Tissue Organ Culture. 2004; 79:63–69.
33. Sarvestani AS, He X, Jabbari E. Viscoelastic characterization and modeling of gelation kinetics of injectable in situ cross-linkable poly(lactide-co-ethylene oxide-co-fumarate) hydrogels. Biomacromolecules. 2007; 8:406–415. [PubMed: 17253761]
34. Rey A, Freire JJ, Bishop M, Clarke JHR. Radius of gyration and viscosity of linear and star polymers in different regimes. Macromolecules. 1992; 25:1311–1315.
35. Jabbari E, He X. Synthesis and characterization of bioresorbable in situ crosslinkable ultra low molecular weight poly(lactide) macromer. J Mater Sci Mater Med. 2008; 19:311–318. [PubMed: 17597374]
36. Jabbari E, He X, Valarmathi MT, Sarvestani AS, Xu W. Material properties and bone marrow stromal cells response to In situ crosslinkable RGD-functionlized lactide-coglycolide scaffolds. J Biomed Mater Res A. 2009; 89:124–137. [PubMed: 18431754]
37. Silverstein, RM.; Bassler, GC.; Morrill, TC. Spectrometric identification of organic compounds. New YorK: John Wiley; 1991. p. 91
38. Kim JW, Ko JY, Suh KD. A useful poly(ethylene oxide)-poly(propylene oxide)- poly(ethylene oxide) triblock crosslinker in a diffusion-controlled polymerization method. Macromol Rapid Commun. 2001; 22:257–261.
39. Odian, G. Principles of polymerization. New York: John Wiley; 1981.
40. Wang J, Ugaz VM. Using in situ rheology to characterize the microstructure in photopolymerized polyacrylarnide gels for DNA electrophoresis. Electrophoresis. 2006; 27:3349–3358. [PubMed: 16892481]
41. Potoczek M, Zawadzak E. Initiator effect on the gelcasting properties of alumina in a system involving low-toxic monomers. Ceramics Int. 2004; 30:793–799.
42. Nowers JR, Costanzo JA, Narasimhan B. Structure-property relationships in acrylate/epoxy interpenetrating polymer networks: Effects of the reaction sequence and composition. J Appl Polym Sci. 2007; 104:891–901.
43. Flory PJ, Rehner J. Statistical mechanics of cross-linked polymer networks I. Rubberlike elasticity. J Chem Phys. 1943; 11:512–520.
44. He ZQ, Xiong LZ. A comparative study on in vitro degradation behaviors of poly(Llactide- co-glycolide) scaffolds and films. J Macromol Sci - Physics. 2010; 49:66–74.

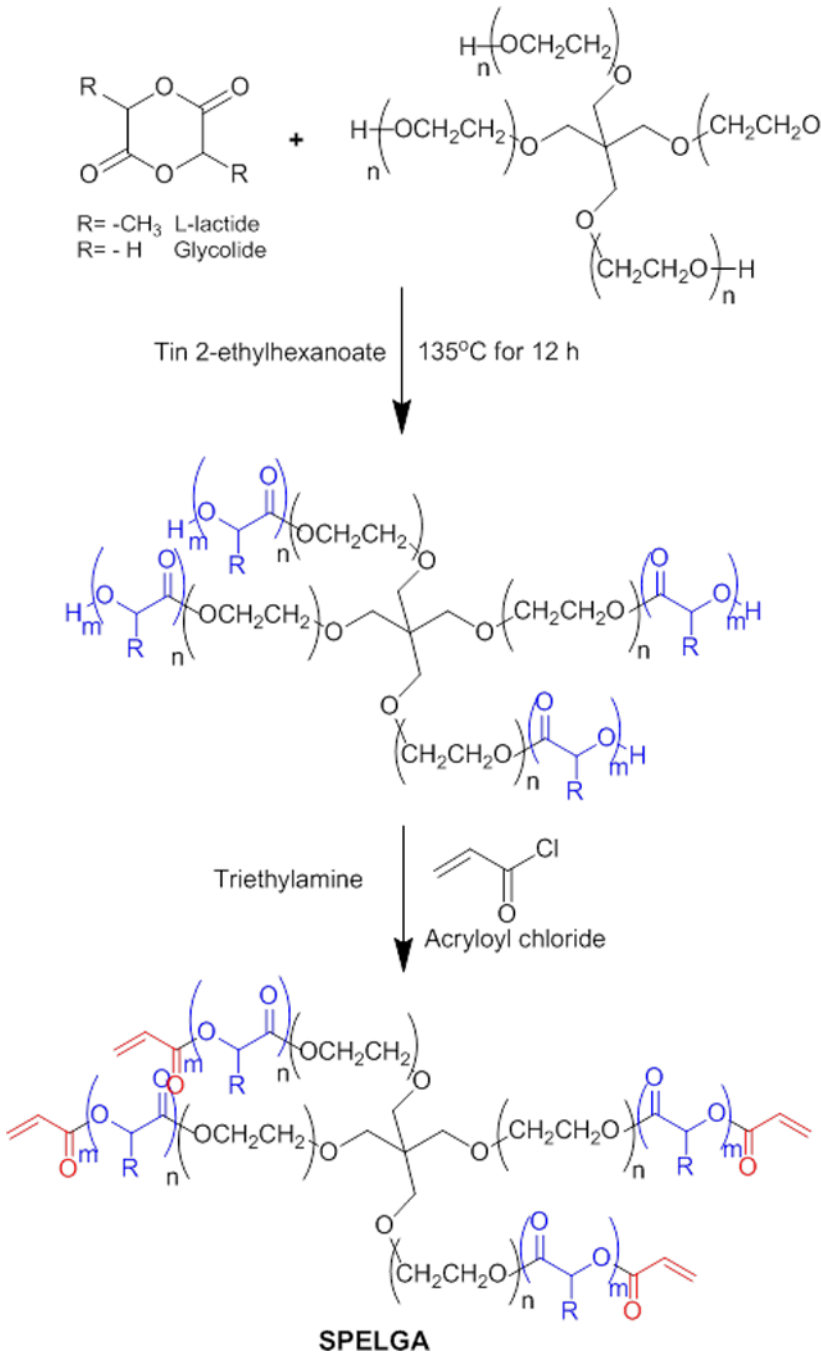

Figure 1.
Reaction scheme for the synthesis of SPELGA macromonomer. The 4-arm PEG, lactide-co-glycolide segments, and terminal acrylate groups are shown by black, red, and blue colors, respectively.

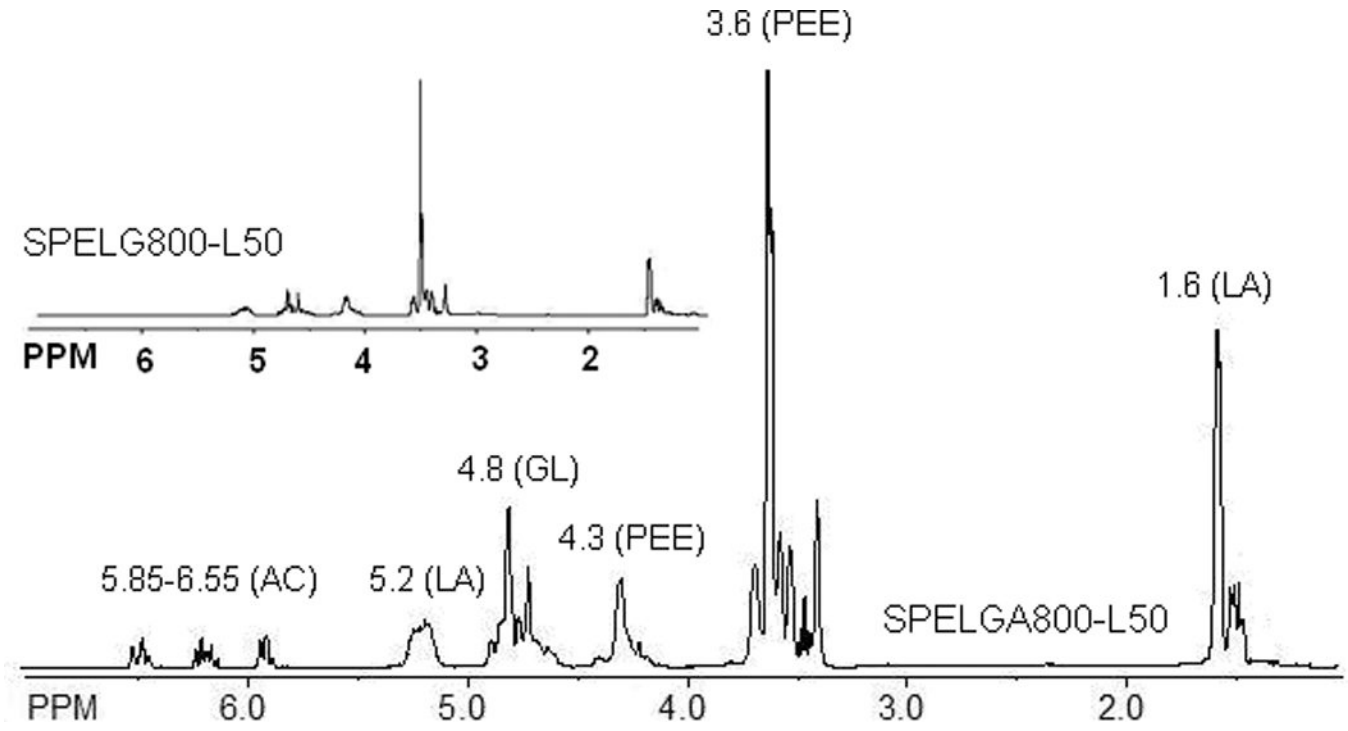

Figure 2.
NMR spectra for SPELGA800-L50. The inset is the spectra of SPELG800-L50 before acrylation.

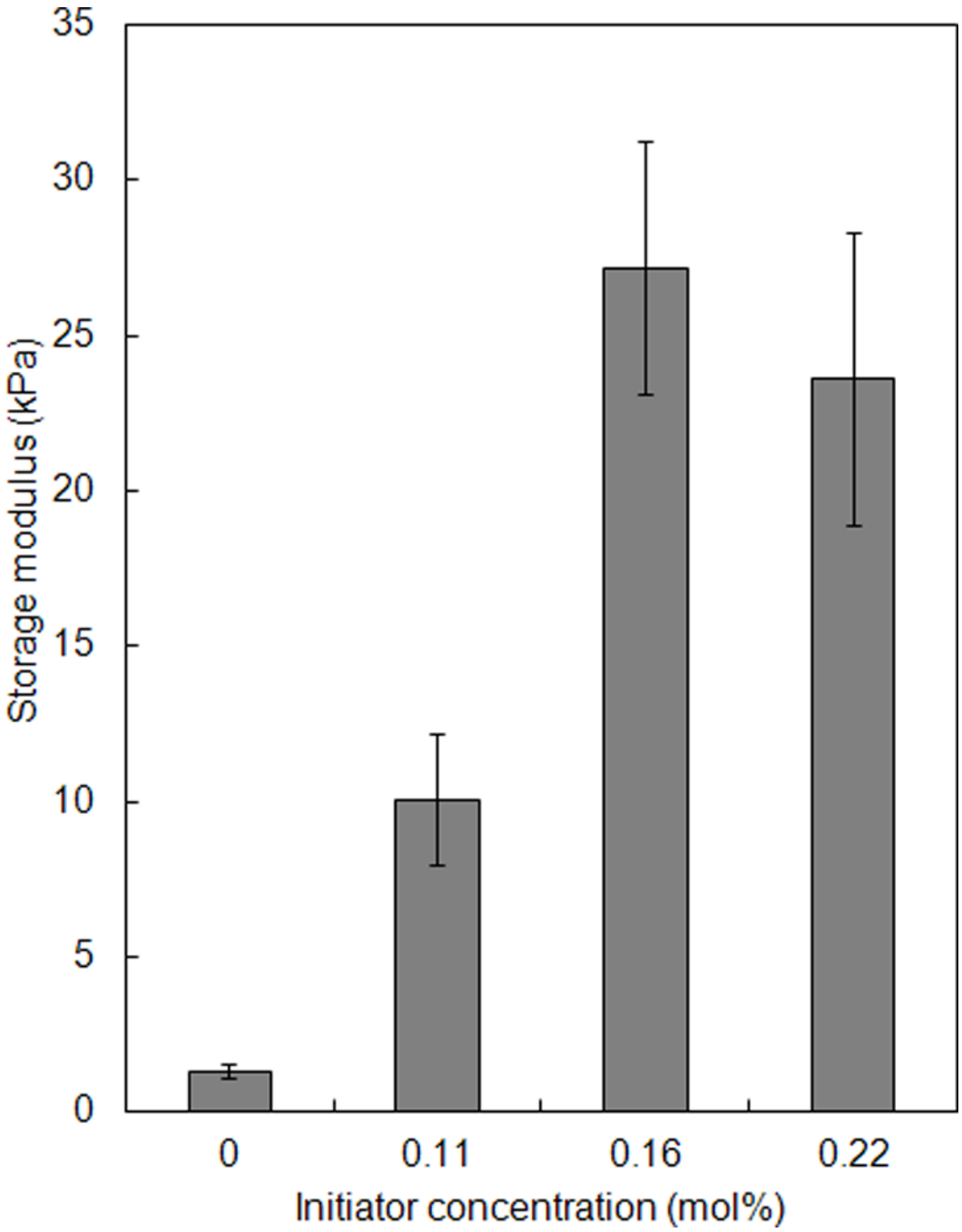

Figure 3.
The effect of UV initiator concentration on shear storage modulus of SPELGA5K-L100-M25-N0 hydrogels. The intensity, distance from the sample, and exposure time of the UV radiation were 46,000 μW/cm^2, 10 cm, and 1800 s, respectively. Values are the mean of three samples with error bars representing one standard deviation from the mean.

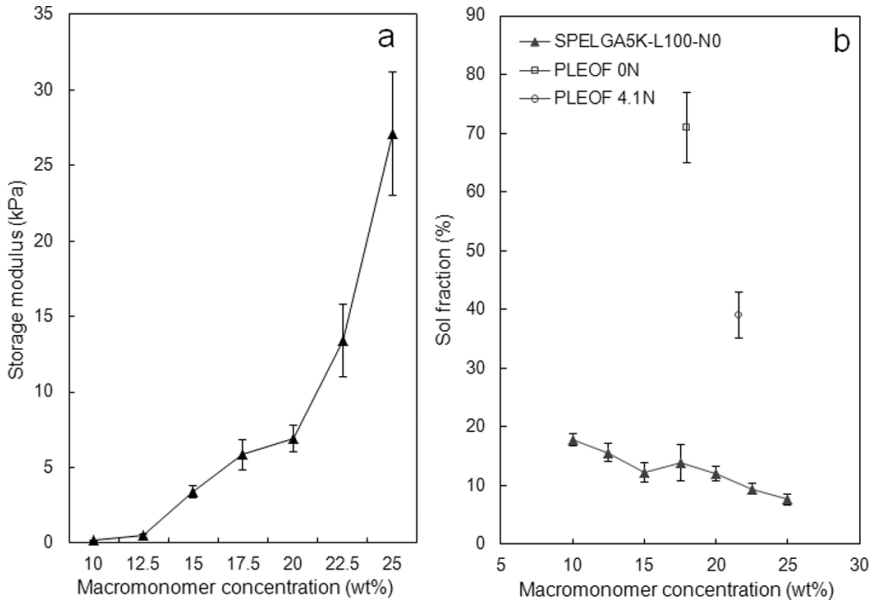

Figure 4.

The effect of macromonomer concentration on the modulus (a) and sol fraction (b) of SPELGA5K-L100-N0-I0.16 hydrogel. The open square and open circle in (b) are the sol fractions of PLEOF hydrogels crosslinked without (17.5% macromonomer) and with (21% macromonomer) 4.1 mol% NVP crosslinker, respectively. The intensity, distance from the sample, and exposure time of the UV radiation were 46,000 μW/cm^2, 10 cm, and 1800 s, respectively. Values are the mean of three samples with error bars representing one standard deviation from the mean.

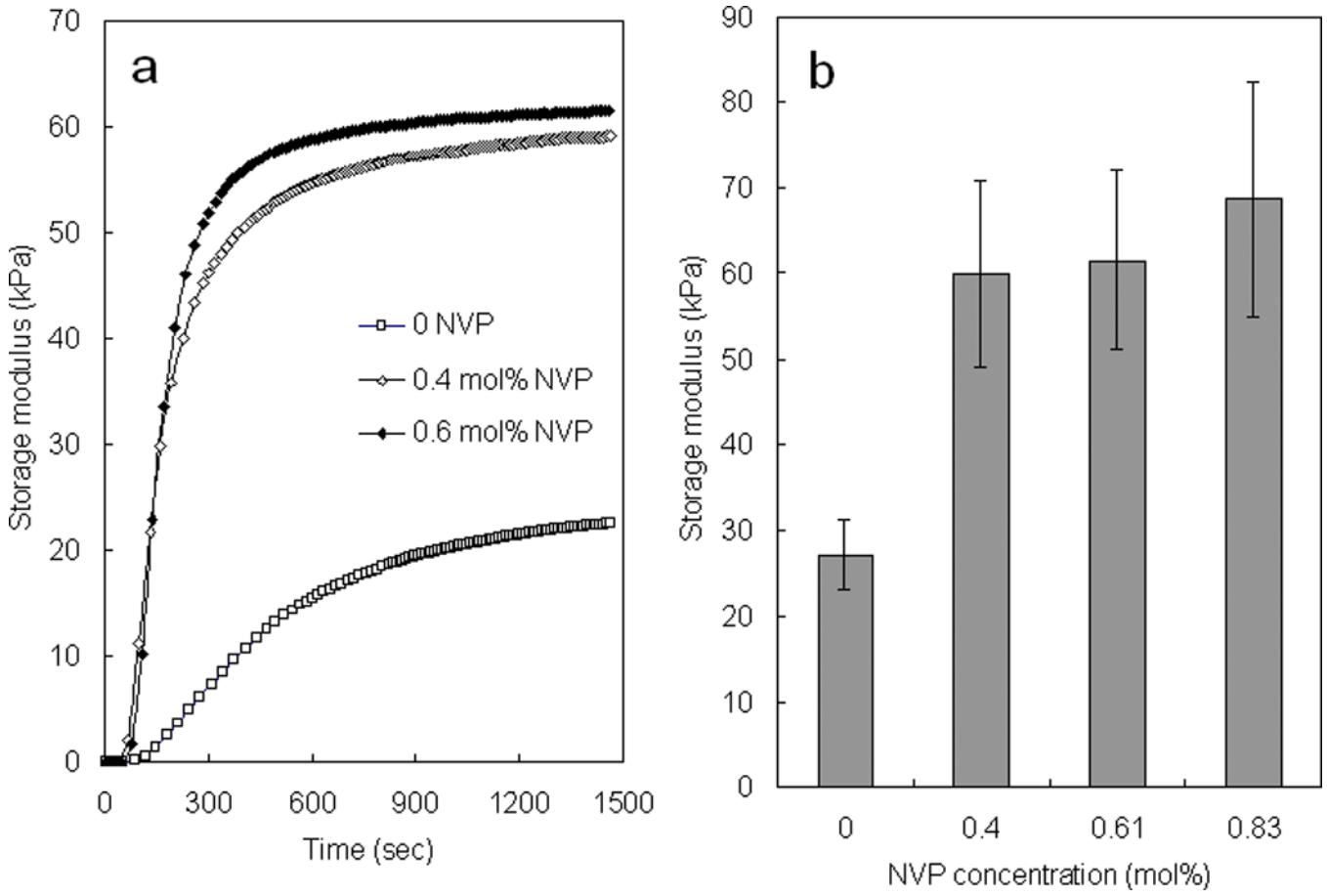

Figure 5.

The effect of NVP monomer concentration on (a) evolution and (b) plateau shear storage modulus of SPELGA5K-L100-M25-I0.16 hydrogels. The intensity, distance from the sample, and exposure time of the UV radiation were 46,000 μW/cm^2, 10 cm, and 1800 s, respectively. Values are the mean of three samples with error bars representing one standard deviation from the mean.

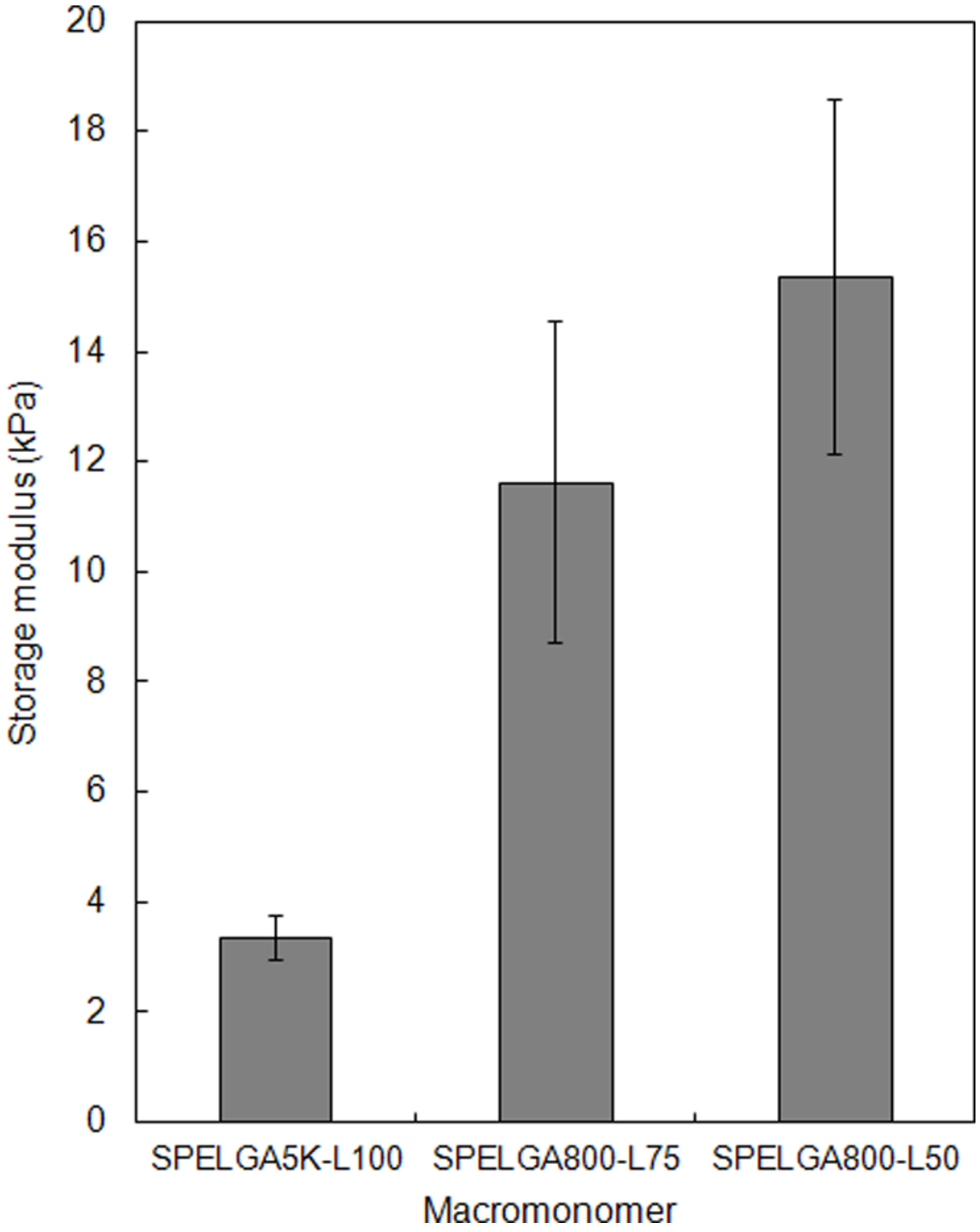

Figure 6.

The effect of initiator molecular weight and LA/GL ratio of SPELGA macromonomer on shear storage modulus of SPELGA-M15-N0-I0.16 hydrogels. The intensity, distance from the sample, and exposure time of the UV radiation were 46,000 μW/cm^2, 10 cm, and 1800 s, respectively. Values are the mean of three samples with error bars representing one standard deviation from the mean.

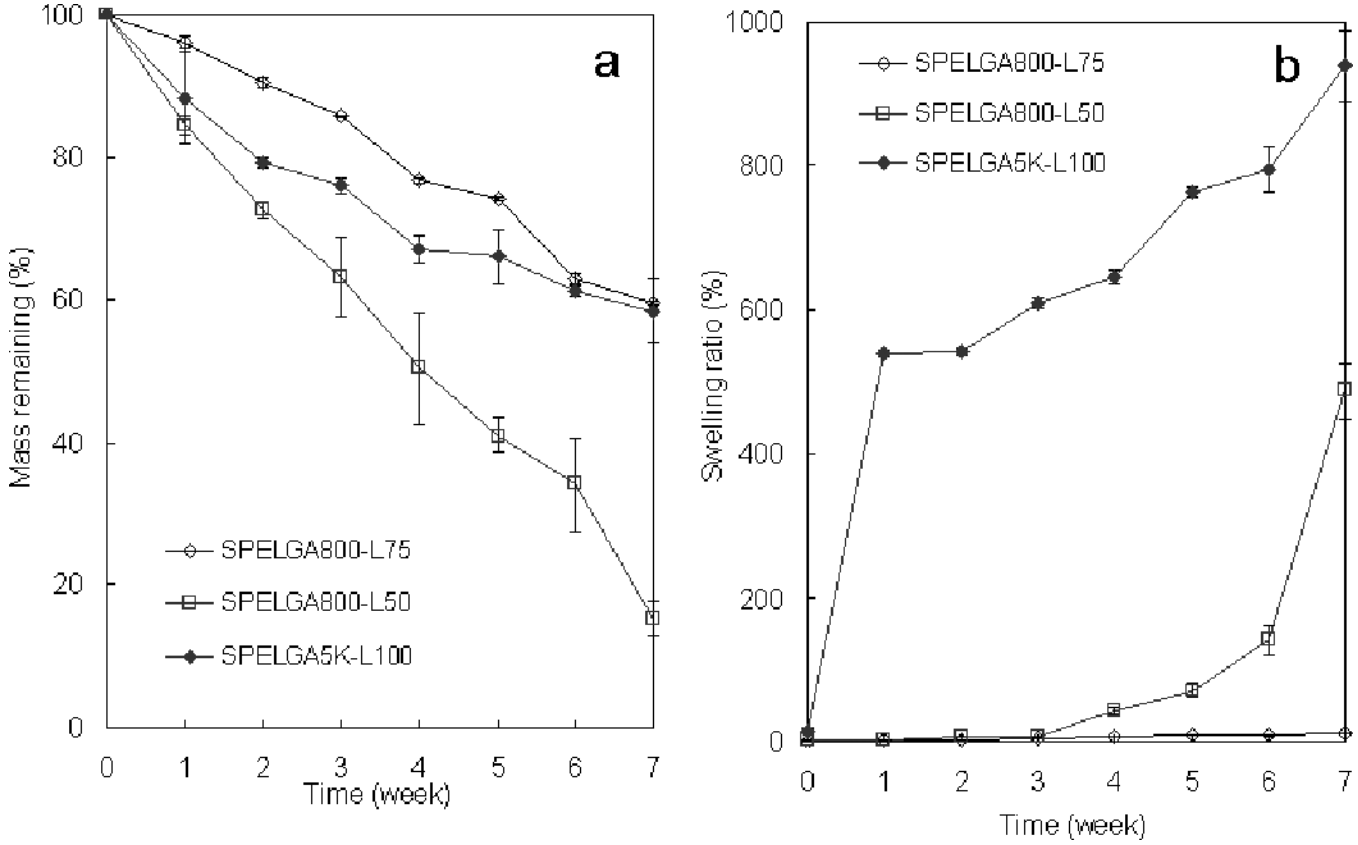

Figure 7.

The effect of initiator molecular weight and LA/GL ratio of SPELGA macromonomer on (a) mass loss and (b) swelling ratio of SPELGA-N0-I0.16 hydrogels. The intensity, distance from the sample, and exposure time of the UV radiation were 46,000 μW/cm^2, 10 cm, and 1800 s, respectively. Values are the mean of three samples with error bars representing one standard deviation from the mean.

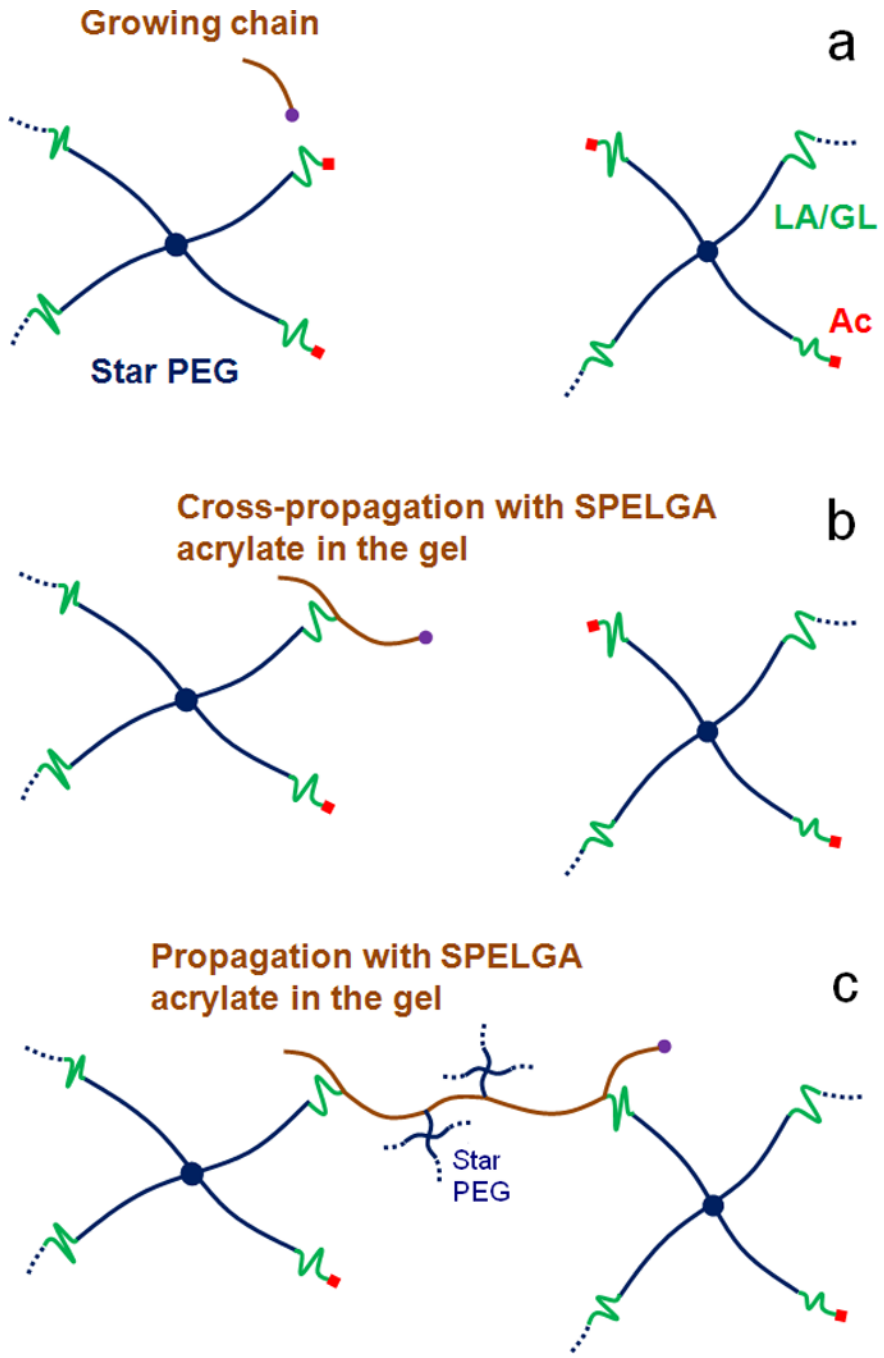

Figure 8.

Schematic diagram to illustrate the cross-propagation reaction of the polymer chains in the sol with network-bound SPELGA acrylates to facilitate crosslinking: scheme a) SPELGA macromonomer with PEG (blue), LA/GL (green), and acrylate (red) groups; the growing polymer chain is shown with a purple dot at the chain end; scheme b) a growing chain in the sol (~X^*) cross-propagates by reaction with a network-bound SPELGA acrylate (>AC; reaction 9) followed by propagation with SPELGA and NVP monomers (reactions 6 and 7) to form a propagating chain bound to the gel; scheme c) the growing chain in the gel cross-propagates with a network-bound SPELGA acrylate to form a load-bearing network chain

(reaction 11). Some SPELGA macromonomers (4-arm blue stars) are shown with a smaller size for clarity.

Table 1

Relative intensity of the chemical shifts in the NMR spectra of SPELGA macromers.

NMR shift (ppm) / Macromonomer (LA/GL feed)	5.85–6.55	5.16	4.77	4.28	3.64	1.56	LA/GL (NMR)	$\overline{M_n}$ (NMR)	# of acrylates/ Macromonomer (NMR)
PLGA800-L50	---	1.0	2.42	1.52	6.03	1.82	1.2	1910	---
PLGAA800-L50	2.93	3.52	9.73	3.51	18.05	8.03	1.2	2260	3.2
PLGAA800-L75	2.96	5.64	5.41	3.41	15.81	12.61	3.4	2600	3.6

Table 2

$\overline{M_n}$, $\overline{M_w}$, and PI of the synthesized SPELGA macromers.

Macromonomer	$\overline{M_n}$	$\overline{M_w}$	PI
SPELGA800-L50	2490	4460	1.80
SPELGA800-L75	2650	4900	1.85
SPELGA800-L100	2640	4400	1.70
SPELGA5K-L100	6570	9460	1.40